  Bull. Chem. Soc. Jpn., 61, 1903—1909 (1988)

Optical Absorption by Mn^{2+} Ions in $MnM(edta)\cdot 6H_2O$ (M=Zn, Cu, Ni, and Co)

Hisashi Togashi,*,† Norimichi Kojima, Toshiro Ban, and Ikuji Tsujikawa
Department of Chemistry, Faculty of Science, Kyoto University, Kyoto 606
(Received Decembder 9, 1987)

The optical absorption spectra of the Mn^{2+} ion in $MnM(edta)\cdot 6H_2O$ (M=Zn, Cu, Ni, and Co) were measured at low temperature. Fine structural bands corresponding to the $^6A_{1g}\rightarrow{}^4T_{2g}$ (D) and $^6A_{1g}\rightarrow{}^4A_{1g}$, ^4E_g (G) transitions were found. The fine structure corresponding to the $^6A_{1g}\rightarrow{}^4A_{1g}$, ^4E_g (G) transition in the Zn compound were analyzed with the ligand field theory and the assignment of the absorption peaks was performed. Although the spectra of the Zn, Cu, and Co compounds are similar, those of the Ni compounds show significant broadening, which is possibly due to the energy transfer caused by the overlapping of the absorption bands of the Ni^{2+} and Mn^{2+}ions.

Recently, bimetallic chelate complexes M′M″ (edta)·$6H_2O$ (M′,M″=metal elements in the 4th period, H_4edta= ethylenediaminetetraacetic acid) were synthesized[1,2] and their magnetic properties have been extensively studied.[3-6] It is because they are good models of one-dimensional ferrimagnets.

One can obtain large variety of isomorphous compounds with different magnetic interaction. In these crystals $[M'(H_2O)_4]^{2+}$ and $[M''(edta)]^{2-}$ are alternately bonded by the carboxyl group of the edta, hence bimetallic chains are formed.

The authors think that these compounds are suitable not only for the magnetic studies but also for the study on the interaction between the electronic states in different metal ions. Such studies have been practiced mainly on the crystals doped with foreign metal ions. However the spectra of the electronic transitions in such materials usually suffer inhomogeneous broadening, which is caused by the difference of the energy levels among the impurity sites. On the contrary, the spectra of M′M″ (edta)·$6H_2O$ will be free from inhomogeneous broadening because these compounds are pure crystals. Visible reflectance spectra of M′M″ (edta)·$6H_2O$ at room temperature were already measured by Escrivá et al.[7]

We prepared single crystals of $MnM(edta)\cdot 6H_2O$(M= Zn, Cu, Ni, and Co) and measured optical absorption spectra at low temperatures, for the purpose to observe the effects of the $[M(edta)]^{2-}$ on the electronic transitions in the $[Mn(H_2O)_4]^{2+}$.

First, preparation of the crystals and the measurement procedure are described. Secondly, the absorption spectra and the corresponding energy levels are discussed on the basis of the ligand field theory. Also we discuss the interaction between $[Mn(H_2O)_4]^{2+}$ and $[M(edta)]^{2-}$.

Experimental

$MnM(edta)\cdot 6H_2O$ (M=Zn, Cu, Ni, and Co) were obtained from the aqueous solution of $MnCl_2\cdot 4H_2O$ (1 mol), Na_2H_2 edta (1 mol), and nitrates or sulfates of M (1 mol) by heating on a water bath. The pH of the solution was adjusted between 5 and 6 by the use of Na_2CO_3 and HNO_3. The precipitated products were refined by recrystallization from water solution. The water solution of the recrystallized material was slowly evaporated at a temperature between 50 and 60 °C and yielded single crystals, of which typical dimension was 3×3×3 mm^3. The colors of the crystals were pale pink (M=Zn), blue (Cu), dark purple (Ni), and dark brown (Co).

It had been found[8] that the crystal structures of Cu and Co salts belong to an orthorhombic system C_{2v}^9-$Pn2_1a$ (Fig. 1). The X-ray diffraction pattern for the powder of our crystals of Cu and Co compounds agreed to these structures. From

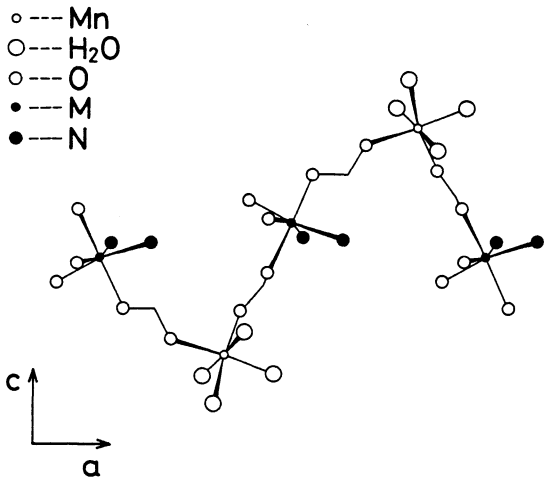

Fig. 1. Schematic view of the structure of MnM(edta)·$6H_2O$ projected on the *ac*-plane. Only metal ions and the atoms which directly coordinate to them are shown.

Table 1. Lattice Constants of $MnM(edta)\cdot 6H_2O$ (M=Zn, Cu, Ni, and Co) with the Space Group of C_{2v}^9-$Pn2_1a$

	a/Å	*b*/Å	*c*/Å
Zn	14.57	13.26	9.84
Cu[a]	14.626	13.068	9.969
Ni	14.40	13.00	9.69
Co[a]	14.584	13.366	9.799

a) Ref. 8.

† Present address: National Chemical Laboratory for Industry, Tsukuba 305.

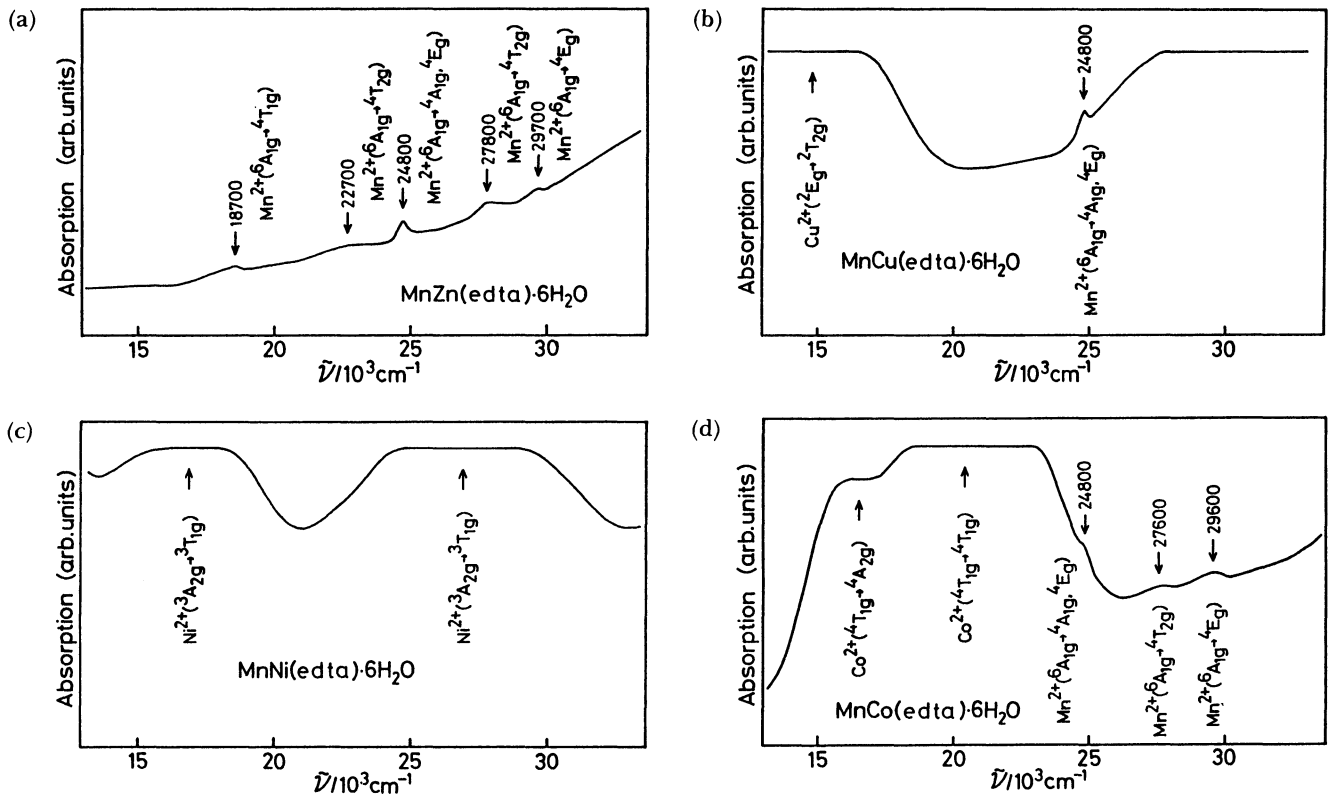

Fig. 2. Unpolarized absorption spectra of MnM(edta)·6H$_2$O at room temperature. a) M=Zn, b) Cu, c) Ni, d) Co.

the diffraction patterns of Ni and Zn compounds, they were found to belong also to the same space group. The lattice constants are shown in Table 1. From the similarity of the crystal parameters and of the spectra, which will be shown in the next section, it is confirmed that, in Ni and Zn compounds, a Mn ion is at the hydrate position and an M ion occupies the chelate position as well as Cu and Co compounds.

In order to measure the absorption spectra, the samples were immersed in liquid helium in a glass dewar. The temperature was lowered by pumping. A spectrometer Jobin-Yvon THR-1500 was used with an iodine lamp, and the electric signal were recorded on chart. When the temperature dependence of the spectra were measured, the samples were hinged to a copper block, with helium gas for heat exchange, sealed in a glass tube immersed in the liquid

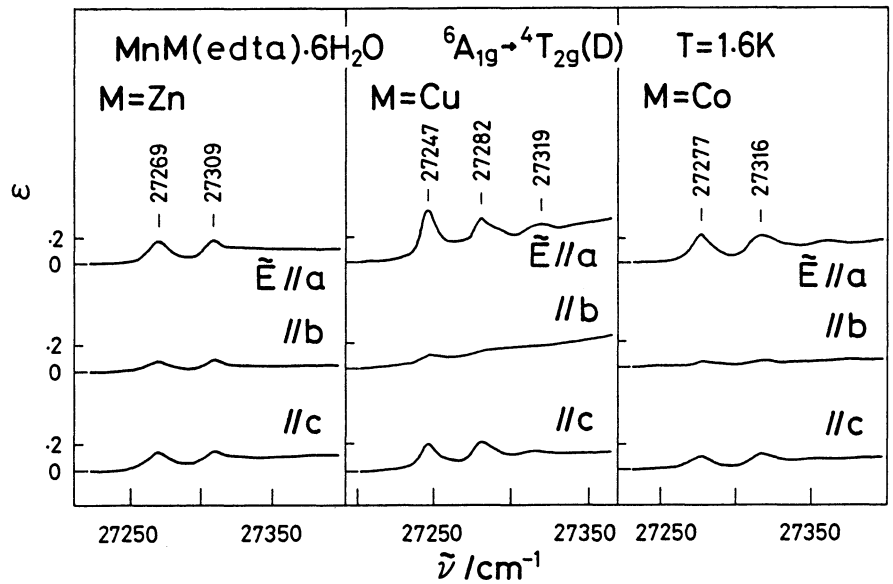

Fig. 3. Absorption spectra corresponding to $^6A_{1g}\rightarrow{}^4T_{2g}(D)$ transition in MnM(edta)·6H$_2$O (M=Zn, Cu, and Co) at 1.6 K.

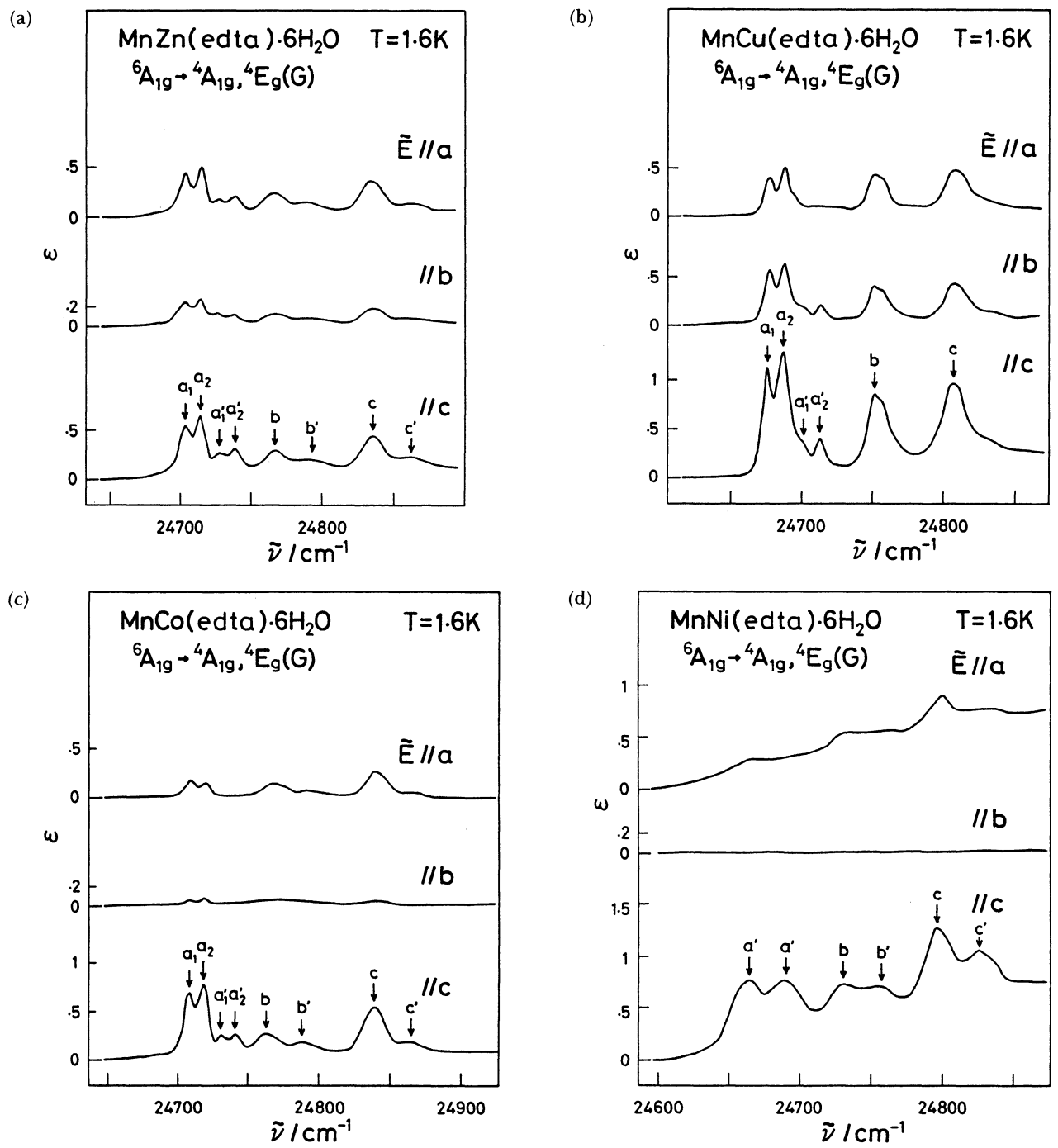

Fig. 4. Absorption spectra corresponding to $^6A_{1g} \rightarrow {}^4A_{1g}, {}^4E_g$ (G) transition in MnM(edta)·6H$_2$O at 1.6 K.
a) M=Zn, b) Cu, c) Co, d) Ni.

helium. The copper block was heated by a manganin coil and its temperature was measured by a germanium and a platinum thermometer.

Results and Discussion

Preliminary measurement of absorption spectra was done at room temperature (Fig. 2). The absorption bands due to spin-allowed transitions in $[M(edta)]^{2-}$ (M=Cu, Ni, and Co) are so strong that most of them were saturated. Some absorption bands due to $[Mn(H_2O)_4]^{2+}$ were found. The assignment of the band peaks in Zn compound is shown in Table 2 (the peak energies agree with the results of Escrivá et al.[7]).

In the absorption spectra of Zn, Cu, Co, and Ni compounds at low temperatures, fine-structural bands were found in two energy regions, 27200—27400 cm^{-1} ($^6A_{1g} \rightarrow {}^4T_{2g}$(D)), and 24600—24900 cm^{-1} ($^6A_{1g} \rightarrow {}^4A_{1g}$, ^4E_g(G)), as shown in Figs. 3 and 4, respectively. Theoretically, the $^4T_{2g}$(D) term consists of 6 Kramers doublets, but we observed only two or three peaks which were separated by about 40 cm^{-1}.

As shown in Fig. 4, the absorption spectra of Zn, Cu,

Table 2. Energy Levels of $MnZn(edta)\cdot 6H_2O$ (in cm^{-1})

Calcd.	Obsd.	
18900	18700	$^4T_{1g}(G)$
22370	22700	$^4T_{2g}(G)$
24780	24800	$^4A_{1g}$, $^4E_g(G)$
27920	27800	$^4T_{2g}(D)$
29750	29700	$^4E_g(D)$
34410		$^4T_{1g}(P)$
40370		$^4A_{2g}$
41540		$^4T_{1g}(F)$
44600		$^4T_{2g}(F)$

$10Dq$=8395, B=710, C=3535.

Table 3. Energies of the Transition $^6A_{1g}\rightarrow{}^4A_{1g}$, $^4E_g(G)$ in $\tilde{E}//c$ Spectra of $MnM(edta)\cdot 6H_2O$ (M=Zn, Cu, Co, and Ni) at 1.6 K (in cm^{-1})

	Zn	Cu	Co	Ni		
a_1	24704	24677	24708			
				24664	$^4A_{1g}(G)$	e_1
a_2	24715	24687	24719			
a_1'	24728	24702s)	24733			
				24690		$e_1+h\nu$
a_2'	24740	24713	24744			
b	24769	24752	24764	24731	$^4E_g(G)$	v
b'	24796s)		24790	24757		$v+h\nu$
c	24835	24806	24838	24798	$^4E_g(G)$	u
c'	24862s)		24864	24827		$u+h\nu$

s) Shoulder.

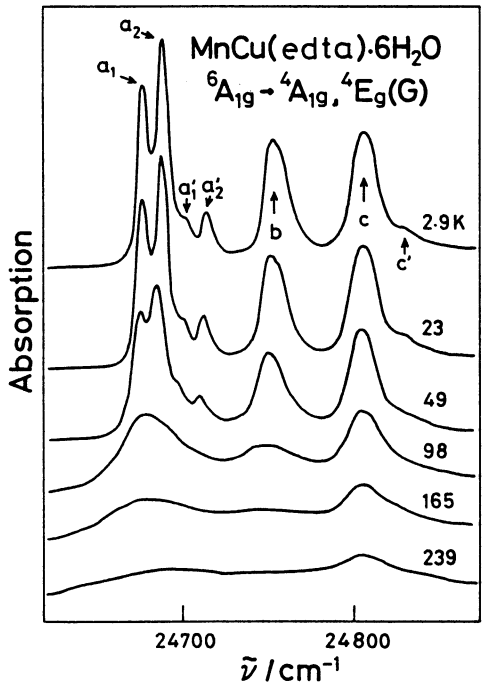

Fig. 5. Absorption spectra corresponding to $^6A_{1g}\rightarrow{}^4A_{1g}$, ^4E_g (G) transition in $MnCu(edta)\cdot 6H_2O$ at various temperatures. The spectra are intentionally shifted to the vertical direction.

and Co compounds in the $^4A_{1g}$, $^4E_g(G)$ region are similar in shape and peak energy. All absorption bands were characterized as due to electric dipole transitions. The absorption spectra can be grouped into three energy regions. We label the peaks and shoulders as shown in the left column of Table 3. The lowest energy region is composed of two peaks (a_1, a_2) associated with weaker peaks at higher energy side (a_1', a_2'); both the middle and the highest energy regions include a rather broad peak (b or c) with a weaker peak lying at higher energy side (b' or c'). For the Co compound the energy differences between a_1 and a_1', a_2 and a_2', b and b', and c and c' are all 25—26 cm^{-1}. Similar tendencies can be seen in the spectra of Zn and Cu compounds. Therefore it is considered that a_1', a_2', b' and c' are the sidebands which originate from a_1, a_2, b and c, respectively and that the elementary excitations corresponding to these sidebands are of the same energy.

In magnetic materials, elementary excitations usually appearing in the optical spectra are phonons and magnons. However, as the present compounds are concerned, the possibility of observing magnon sidebands can be excluded. As Zn^{2+} is not a magnetic ion, it inhibits the interaction between Mn^{2+} ions, then the magnon energy of Zn compound, if any, would be much smaller than the other compounds. Since the phonon energies are expected to be nearly the same because of the similarity in the crystal structure among these compounds, it can be concluded that these sidebands are phonon assisted ones.

The absorption spectra of $^6A_{1g}\rightarrow{}^4A_{1g}$, $^4E_g(G)$ transition in $MnNi(edta)\cdot 6H_2O$ are shown in Fig. 4(d), and the peak energies are listed in Table 3. This energy region is overlapping with the $^3A_{2g}\rightarrow{}^3T_{1g}(P)$ transition band in $[Ni(edta)]^{2-}$ (Ref. 9). In these spectra no splitting was observed for the a band, and the other peaks are also substantially broadened as compared with those in the other compounds. These broadening, of course, is not due to the inhomogeneity of the crystal. Nor does it seem to be due to the significant difference between Ni compound and the other ones in the way that the ligands coordinate to a Mn^{2+} ion, because the crystal parameters seem very similar among these materials (Table 1).

As will be shown later, the absorption hands a, b, and c are due to zero-phonon transitions. The width of a zero-phonon line can be explained[10] by the difference W in curvature between the potential curves for the ground and the excited states. We think that the shape of the potential curves of the $[Mn(H_2O)_4]^{2+}$ is changed, and then the W is increased, because of a resonant transfer of excitons between $^4A_{1g}$ and $^4E_g(G)$ band of $[Mn(H_2O)_4]^{2+}$ and $^3T_{1g}$ band of $[Ni(edta)]^{2-}$. However the elucidation of this phenomenon is the subject for future study.

In order to characterize the excitations corresponding to the absorption lines a_1, a_2, b, and c, we measured the temperature dependence of the absorption spectra of the Cu compound (Fig. 5). Since this compound

has the smallest sideband intensity among the three compounds, we thought that the overall intensity of the absorption in this region can be a good measure for the sum of the intensities of these peaks. The result shows the decrease of the intensity with increasing temperature (Fig. 6). This tendency is characteristic of pure electronic transitions. We analyzed the intensity change quantitatively, using an equation for the intensity of a zero-phonon transition line,[11] with the assumption that the excited state and the ground state have the potential curves of the same shape but the energies at their minima do not necessarily coincide. Also we assume that only one kind of phonon is involved in the temperature change of the zero-phonon transition. The equation is

$$\ln(I(T)/I_0) = -(E_0/\hbar\omega_0)[\coth(\hbar\omega_0/2kT) - 1], \quad (1)$$

where $I(T)$ is the intensity at temperature T, I_0 the intensity at absolute zero, $\hbar\omega_0$ the energy of the phonon involved, and E_0 is the Stokes energy loss due to the mutual displacement of the curve minima. Parameters were obtained as E_0=65 cm^{-1}, $\hbar\omega_0$=123 cm^{-1} by the least squares method (Fig. 6).

The value of $\hbar\omega_0$ seems to be overestimated, because the temperature change of absorption intensity due to phonons is usually dominated by the phonon of lowest energy, and, as we already know, the 25 cm^{-1} phonon also exists in MnCu(edta)·6H$_2$O. This overestimation can be explained from the fact that the values of E_0 and $\hbar\omega_0$ are very sensitive to mixing of other bands (like phonon sidebands) with the intensity I. It is probable that phonon sidebands overlaps the bands of the zero-phonon transition, especially at higher temperatures. Nevertheless, the negative temperature dependence of the intensity of the origin peaks indicates that they are due to zero-phonon transitions.

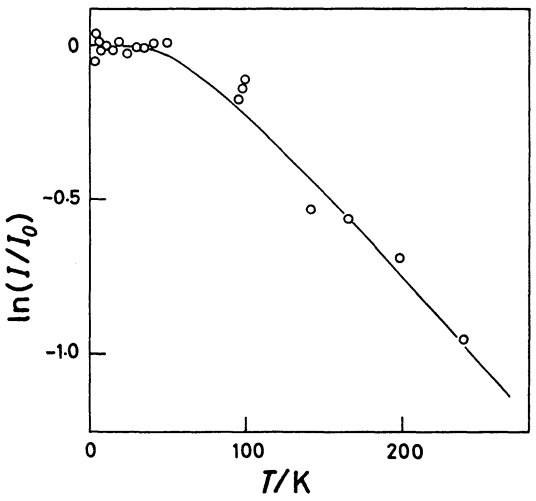

Fig. 6. Temperature dependence of the intensity of the absorption corresponding to the $^6A_{1g} \rightarrow {}^4A_{1g}, {}^4E_g$ (G) transition in MnCu(edta)·6H$_2$O. The solid line is the best fit one calculated from Eq. 1.

Next, we assign the a_1, a_2, b, and c peaks of MnZn(edta)·6H$_2$O to the 6 Kramers doublets of the $^4A_{1g}$, ^4E_g(G) terms. In the unit cell all sites of the Mn^{2+} ions are equivalent,[8] therefore all Mn^{2+} ions have the same energy levels.

In order to calculate the energy levels of the components in $^4A_{1g}$(G) and ^4E_g(G), it is necessary to obtain ligand field parameters[12] Dq, B, and C. As described previously a Mn^{2+} ion is coordinated by 4 water molecules and 2 carboxyl groups, forming a distorted octahedron. We calculated the ligand field parameters of this octahedron, using the room temperature data in Table 2, with the least squares method. The calculated energy levels are shown in the same table. These values, 10Dq=8395, B=710, and C=3535 cm^{-1}, are very close to the parameters for $[Mn(H_2O)_6]^{2+}$, 10Dq=8480, B=671, and C=3710 cm^{-1} (Ref. 13). This similarity seems to agree with the fact that $C_2O_4^{2-}$ is placed near H_2O in the spectrochemical series.

In coordination compounds of transition metal ions, in general, the most significant factor in lifting the degeneracy of the energy levels of a term ($^{2S+1}\Gamma$) is the ligand field of symmetry lower than cubic. As the site symmetry of Mn^{2+} ion in the MnM(edta)·6H$_2$O is 1, all kinds of lower symmetry fields, in some degree, contribute to the splitting. It seems that the largest contribution is from the ligand field of C_{2v} symmetry, because it is the highest symmetry a *cis*-MA_4B_2 cluster can have.

We approximate the cluster, $[Mn(H_2O)_4]^{2+}$ with two carboxyl groups, as *cis*-MA_4B_2 with C_{2v} symmetry. For the sake of calculation we define a cartesian coordinate system as follows: The direction of the linearly arranged A-M-A coincide with the z-axis and that the 2-fold axis of C_{2v} coincides with the $x+y$ axis. Also the one-particle wave functions of t_2 and e electrons are defined in the way that, under symmetry operations, wave functions ξ, η, and ζ of t_2 electrons are transformed like yz, zx, and xy, respectively, and u and v of e electrons behave like $3z^2-r^2$ and x^2-y^2, respectively.

When the potential V_0 of C_{2v} symmetry is expanded with r_i, which is the position vector of an i-th electron with its origin at the center of the metal ion, we obtain

$$V_0 = V_{cub} + V_{\alpha+\beta}^{(1)}(T_{1u}) + V_u^{(2)}(E_g) + V_\zeta^{(2)}(T_{2g}) + V_{\alpha+\beta}^{(3)}(T_{1u}) + V_u^{(4)}(E_g) + V_\zeta^{(4)}(T_{2g}) + (\text{higher order terms}), \quad (2)$$

where $V_{cub}=\sum v_{cub}(r_i)$ represents the cubic field potential, $V_\gamma^{(n)}(\Gamma_p)=\sum v_\gamma^{(n)}(\Gamma_p, r_i)$is a nth-order potential operator which is the γ component of an irreducible representation Γ of the cubic point group O_h, and p(=g, u) denotes the parity of the potential.

It is known that all the one-electron matrix elements among the $^4A_{1g}$, ^4E_g(G), and ^4E_g(D) levels are zero, Then, in order to lift the degeneracy of the $^4A_{1g}$ and ^4E_g(G), it is necessary to consider $^4T_{1g}$ and $^4T_{2g}$ terms.

Since the potential operators of odd parity are not important, we can assume that a perturbation Hamiltonian $V_L=V_\zeta^{(2)}$ (T_{2g}), neglecting the higher order terms than the second.

The wave functions of $^4A_{1g}$, $^4E_g(G)$, $^4T_{1g}$'s, and $^4T_{2g}$'s are described as

$$\psi(^4A_{1g}\, e_1\, 3/2)=(30)^{-1/2}\,(3|\xi\eta\zeta u\bar{v}|+3|\xi\eta\zeta\bar{u}v|-2|\bar{\xi}\eta\zeta uv|-2|\xi\bar{\eta}\zeta uv|-2|\xi\eta\bar{\zeta}uv|)$$

$$\psi(^4E_g(G)\, u3/2)=(42)^{-1/2}\,(4|\xi\eta\bar{\zeta}uv|-2|\xi\bar{\eta}\zeta uv|-2|\bar{\xi}\eta\zeta uv|-3|\xi\eta\zeta u\bar{v}|+3|\xi\eta\zeta\bar{u}v|)$$

$$\psi(^4E_g(G)\, v3/2)=(14)^{-1/2}\,(2|\bar{\xi}\eta\zeta uv|-2|\xi\bar{\eta}\zeta uv|-\sqrt{3}|\xi\eta\zeta u\bar{u}|+\sqrt{3}|\xi\eta\zeta v\bar{v}|)$$

$$\psi(^4T_{1g}{}^n\,\gamma\,3/2)=-\lambda_n|\xi\eta\bar{\zeta}\zeta u|-(\mu_n/\sqrt{2})\,(|\zeta\xi\bar{\xi}uv|+|\zeta\eta\bar{\eta}uv|)+\nu_n|\xi\eta uv\bar{v}|$$

$$\psi(^4T_{2g}{}^n\,\zeta\,3/2)=l_n|\xi\eta\bar{\zeta}\zeta v|+(m_n/\sqrt{2})\,(|\zeta\xi\bar{\xi}uv|-|\zeta\eta\bar{\eta}uv|)-n_n|\xi\eta vu\bar{u}|$$

(n=1, 2, and 3),

where superscripts n=1, 2, and 3 of $^4T_{1g}{}^n$ denote G, P, and F terms, respectively, and those of $^4T_{2g}{}^n$ correspond to G, D, and F, respectively, and the parameters λ_n, μ_n, ν_n, l_n, m_n, and n_n were obtained simultaneously with the determination of Dq, B, and C (Table 4).

The matrix elements of the $V_L=V_\zeta^{(2)}$ (T_{2g}) between ($^4A_{1g}$, $^4E_g(G)$) and ($^4T_{1g}$' s, $^4T_{2g}$'s) are expressed as

$$\langle ^4T_{2g}{}^n\,\zeta|V_L|^4E_g(G)\,u\rangle=(1/3\sqrt{14})\,(n_n-l_n)\langle e||v_\zeta^{(2)}(T_{2g})||t_2\rangle$$

$$\langle ^4T_{1g}{}^n\,\gamma|V_L|^4E_g(G)\,v\rangle=(1/\sqrt{42})\,[\sqrt{3}(\nu_n-\lambda_n)\langle e||v_\zeta^{(2)}(T_{2g})||t_2\rangle+4\mu_n\langle t_2||v_\zeta^{(2)}(T_{2g})||t_2\rangle]$$

$$\langle ^4T_{2g}{}^n\,\zeta|V_L|^4A_{1g}\,e_1\rangle=(\sqrt{5/3}\sqrt{2})\,(l_n-n_n)\langle e||v_\zeta^{(2)}(T_{2g})||t_2\rangle.$$

(n=1, 2, and 3)

The other matrix elements are zero.

The irreducible matrix elements $\langle t_2||v_\zeta^{(2)}(T_{2g})||t_2\rangle$ and $\langle e||v_\zeta^{(2)}(T_{2g})||t_2\rangle$ are equal to $\sqrt{6}\langle\zeta|v_\zeta^{(2)}(T_{2g})|\eta\rangle$ and $\sqrt{3}\langle u|v_\zeta^{(2)}(T_{2g})|\zeta\rangle$, respectively. For convenience, we approximate that

$$\langle t_2||v_\zeta^{(2)}(T_{2g})||t_2\rangle=-(3/2)^{1/2}\langle e||v_\zeta^{(2)}(T_{2g})||t_2\rangle,$$

which exactly holds when the field around the Mn^{2+} ion is spherically symmetric.

Table 4. The Coefficients λ_n,μ_n, and ν_n for $^4T_{1g}{}^n$ and l_n, m_n, and n_n for $^4T_{2g}{}^n$ in MnZn(edta)·$6H_2O$

	n=1	2	3
λ_n	0.977	−0.053	−0.207
μ_n	−0.125	0.643	−0.755
ν_n	0.173	0.764	0.622
l_n	0.843	−0.437	−0.312
m_n	0.441	0.895	−0.062
n_n	0.307	−0.085	0.948

By Koide and Pryce,[14] it has been shown that the difference in covalency between t_2 and e electrons can separate the $^4A_{1g}$ and $^4E_g(G)$ terms, even if the Mn^{2+} ion is in no lower symmetry field than cubic. Therefore we take into account the effect of the covalency by introducing a parameter Δ, which is defined as

$$\Delta\equiv E_0(^4E_g(G))-E_0(^4A_{1g}),$$

where $E_0(\Gamma)$ is the energy of a Γ term in the cubic field.

The covalency effect (Δ) and the low symmetry field (V_L) combine to separate the $^4A_{1g}$, $^4E_g(G)$ term into three states; $^4A_{1g}e_1$, $^4E_g(G)u$, and v. Furthermore each state is split into two Kramers doublets by spin-orbit interaction V_{so}, which will explain the energy difference between the a_1 and a_2 absorption lines. In the estimation of the magnitude of the spin-orbit interaction for the $^4A_{1g}$ and ^4E_g states, the effect of the α and the β components of the $^4T_{1g}{}^n$ and the ξ and the η components of the $^4T_{2g}{}^n$ can be neglected, because, they contribute, at the most, to the energies of $^4A_{1g}$, $^4E_g(G)$ through terms like

$$|\langle ^4\Gamma e|V_{so}|^4T\delta\rangle|^2/[E_0(^4\Gamma)-E_0(^4T)],$$

where $^4\Gamma e$ is the general expression of the components of the $^4A_{1g}$ and $^4E_g(G)$ terms and $^4T\delta$ represents $^4T_{1g}{}^n\alpha$, β and $^4T_{2g}{}^n\xi$, η. On the other hand, $^4T_{1g}{}^n\gamma$ and $^4T_{2g}{}^n\zeta$ contribute through terms like

$$\langle ^4\Gamma e|V_L|^4T\psi\rangle\langle ^4T\psi|V_{so}|^4\Gamma e\rangle/[E_0(^4\Gamma)-E_0(^4T)],$$

where $^4T\psi$ denotes $^4T_{1g}{}^n\gamma$ or $^4T_{2g}{}^n\zeta$.

Therefore, the matrix elements which will significantly contribute to the splitting are calculated as

$$\langle ^4T_{1g}{}^n\,\gamma\,M|V_{so}|^4A_{1g}\,M\rangle=-(i/3\sqrt{15})\,[\sqrt{2}(\lambda_n-\nu_n)\,\zeta'+4\mu_n\zeta]M$$

$$\langle ^4T_{1g}{}^n\,\gamma\,M|V_{so}|^4E_g(G)\,u\,M\rangle=-(i/3\sqrt{21})\,[\sqrt{2}(\lambda_n-\nu_n)\,\zeta'+4\mu_n\zeta]M$$

$$\langle ^4T_{2g}{}^n\,\zeta\,M|V_{so}|^4E_g(G)\,v\,M\rangle=(i\sqrt{2}/\sqrt{21})\,(l_n-n_n)\,\zeta' M$$

(M=3/2, 1/2, −1/2, −3/2),

where $\zeta=(-i/3)\langle t_2||v_{so}||t_2\rangle$ and $\zeta'=(i/3\sqrt{2})\langle t_2||v_{so}||e\rangle$. We use the spherical-symmetry approximation also for the spin-orbit interaction parameters, in which $\zeta=\zeta'$.

With the use of the matrix elements obtained above, the energy levels of the $|^4A_{1g}\,e_1\,M\rangle$, $|^4E_g(G)\,u\,M\rangle$, and $|^4E_g(G)\,v\,M\rangle$ ($M=\pm3/2,\ \pm1/2$) can be calculated. Neglecting the non-diagonal matrix elements between different spin states, we can reduce the secular equation of V_L+V_{so} between 36 components of $^4A_{1g}e_1$, ^4E_gu, and v, $^4T_{1g}{}^n\gamma$, $^4T_{2g}{}^n\zeta$ (n=1, 2, and 3) into 4 equations, each one corresponding to each spin state M. Because Kramers degeneracy still remains, we have to consider only two of them, e.g. those for M=3/2 and 1/2. We fixed the parameter ζ at 347 cm^{-1}, which is the value for a free Mn^{2+} ion, and adjusted the $\langle e||v_\zeta^{(2)}$

$(T_{2g})||t_2>$ and the Δ so as to fit the average energy of each state, $^4A_{1g}e_1$, $^4E_g u$, and v, to the corresponding one observed.

We obtained $<e||v_\zeta^{(2)}(T_{2g})||t_2>=1257$ and $\Delta=125$ cm^{-1}, and found that the (a_1, a_2), b and c bands correspond to the $^4A_{1g}$ e_1, ^4E_g v, and u states, respectively (Table 2). In the theory of Koide and Pryce, the effect of the covalency is taken into account by mixing the σ-orbitals of the ligands with those of the e-orbitals of the metal ion. The observed value of the Δ is a little larger than the theoretical upper limit, $\Delta=114.5$ cm^{-1}, which were estimated from the values of B and C. For the other compounds of Mn^{2+}, it was found[15] that a spin-doublet state situated near this energy region can influence the energy levels of the components of $^4A_{1g}e_1$, $^4E_g(G)u$, and v. Therefore it is possible that the calculated value of the Δ in MnZn (edta)·6H_2O is increased by the effect of a doublet state.

The calculated splittings of the $^4A_{1g}e_1$, $^4E_g(G)v$, and u due to the spin-orbit interaction are 4.6, 1.0, and 0.0 cm^{-1}, respectively. It is also found that the largest contribution to the eigenfunctions of these states is from the ζ components of $^4T_{2g}(G)$ or $^4T_{2g}(D)$ among the $^4T_{1g}$'s and $^4T_{2g}$'s. This result explains the fact that no splitting were observed in the b and c bands. However, for the splitting of the (a_1, a_2), the calculated value is smaller than the observed one. This descrepancy can be explained from the splitting of the $^4T_{2g}(G)$ or $^4T_{2g}(D)$ band due to the low symmetry field V_L; because the energy difference between each of these bands and the $^4A_{1g}$, $^4E_g(G)$ is only about 3000 cm^{-1}, it is possible that the energy shift of the ζ component of the either band toward the $^4A_{1g}$, $^4E_g(G)$ region increase the splitting of the $^4A_{1g}e_1$ state.

Figures 3 and 4 show that the absorption spectra of M=Zn, Cu, and Co compounds are very similar in shape, which implies that the interaction between $[Mn(H_2O)_4]^{2+}$ and $[M(edta)]^{2-}$ is not significant in these spectra.

Conclusion

The absorption spectra corresponding to the electronic transition in Mn^{2+} ion in MnM(edta)·6H_2O (M=Zn, Cu, Ni, and Co) were measured at low temperature.

It was found that the absorption spectra corresponding to the $^6A_{1g}\rightarrow{}^4A_{1g}$, $^4E_g(G)$ transition in Mn^{2+} ions in MnM(edta)·6H_2O (M=Zn, Cu, and Co) are similar to each other; the structure of their energy levels can be explained as caused by the covalency effect and by the interaction from the $^4T_{1g}$'s and $^4T_{2g}$'s through a low symmetry field $V_\zeta(T_{2g})$. The fine structure of the $^4A_{1g}$, $^4E_g(G)$ band in Zn compound was assigned, considering the splitting of the absorption peaks due to the spin-orbit interaction. In MnNi(edta)·6H_2O, although its spectra are similar to those of the other compounds in energy, its line widths are much broader than in the other materials. It seems that this broadening is related to the overlapping of the absorption bands of $[Mn(H_2O)_4]^{2+}$ and $[Ni(edta)]^{2-}$. However, further investigation is needed to solve this problem.

References

1) D. Beltrán and J. Beltrán, *Rev. Acad. Cienc. Exactus, Fis. Quim. Nat. Zaragoza*, **31**, 229 (1976).
2) E. Escrivá, D. Beltrán, and J. Beltrán, *An. R. Soc. Esp. Fis. Quim., Ser. B*, **77**, 330 (1981).
3) D. Beltrán, E. Escrivá, and M. Drillon, *J. Chem. Soc., Faraday Trans. 2*, **78**, 1773 (1982).
4) M. Drillon, E. Coronado, D. Beltrán, and R. Georges, *Chem. Phys.*, **79**, 449 (1983).
5) M. Drillon, E. Coronado, D. Beltrán, J. Curely, R. Georges, P. R. Nugteren, L. J. de Jongh, and J. L. Genicon, *J. Magn. Magn. Mater.*, **54—57**, 1507 (1986).
6) E. Coronado, M. Drillon, A. Fuertes, D. Beltrán, A. Mosset, and J. Galy, *J. Am. Chem. Soc.*, **108**, 900 (1986).
7) E. Escrivá, A. Fuertes, and D. Beltrán, *Transition Met. Chem.*, **9**, 184 (1984).
8) X. Solans, M. Font-Altaba, J. Oliva, and J. Herrera, *Acta Crystallogr., Sect. C*, **39**, 435 (1983).
9) C. K. Jorgensen, *Acta Chem. Scand.*, **9**, 1362 (1955).
10) I. S. Osad'ko, "Spectroscopy and Excitation Dynamics of Condensed Molecular Systems," Chap. 8, ed by V. M. Agranovich and R. M. Hochstrasser, North-Holland, Amsterdam (1983).
11) K. K. Rebane, "Impurity Spectra of Solids," Chap. 2, Plenum Press, New York, (1970).
12) S. Sugano, Y. Tanabe and H. Kamimura, "Multiplets of Transition-Metal Ions in Crystals," Chap. V, Academic Press, New York (1970).
13) L. J. Heidt, G. F. Koster, and A. M. Johnson, *J. Am. Chem. Soc.*, **80**, 6471 (1958).
14) S. Koide and M. H. L. Pryce, *Phil. Mag.*, **3**, 607 (1958).
15) W. van Erk and C. Haas, *Phys. Stat. Sol. (b)*, **70**, 517 (1975).